

Sonochemical Hydrogen Production Efficiently Catalyzed by Au/TiO<sub>2</sub>Yifeng Wang,<sup>†</sup> Dan Zhao,<sup>†</sup> Hongwei Ji,<sup>†</sup> Guilin Liu,<sup>†</sup> Chuncheng Chen,<sup>†</sup> Wanhong Ma,<sup>†</sup> Huaiyong Zhu,<sup>‡</sup> and Jincai Zhao<sup>\*,†</sup>*Key Laboratory of Photochemistry, Beijing National Laboratory for Molecular Sciences, Institute of Chemistry, Chinese Academy of Sciences, Beijing 100080, China, and Inorganic Materials Research Program, School of Physical and Chemical Science, Queensland University of Technology, GPO Box 2434, QLD 4001 Australia**Received: June 21, 2010; Revised Manuscript Received: August 31, 2010*

Au/TiO<sub>2</sub> was used as a highly efficient sonocatalyst to produce H<sub>2</sub> from water or aqueous solutions. Au/TiO<sub>2</sub> significantly increased the yields of H<sup>•</sup> and <sup>•</sup>OH radicals in the sonolysis of water. Product analysis and isotope evidence indicated that hydrogen molecules derived from methanol/water solutions were formed by three pathways: (1) recombination of two H<sup>•</sup> atoms from the cleavage of water molecules, (2) H-abstraction from methanol by H<sup>•</sup> generated by water cleavage, and (3) thermal reforming of methanol. The relative importance of each pathway was assessed by carefully analyzing the hydrogen-isotope composition of the evolved hydrogen gas using a modified gas chromatograph. The source of hydrogen in the H<sub>2</sub> evolved from methanol/water solutions during sonolysis was also addressed. Data showed that, although the addition of methanol in the presence of Au/TiO<sub>2</sub> resulted in a 12-fold increase in the rate of H<sub>2</sub> evolution, nearly half of the hydrogen atoms were nevertheless derived from water molecules. Control studies of H<sub>2</sub> formation in the presence of bare TiO<sub>2</sub> and in the absence of a catalyst were also performed. In both cases, the compositions of evolved hydrogen gas were similar to that of the Au/TiO<sub>2</sub> system, although hydrogen evolution was much slower. These findings reveal that Au nanoparticles on the TiO<sub>2</sub> surface effectively catalyze water cleavage and methanol reforming.

## 1. Introduction

The catalytic properties of gold nanostructured materials have attracted much attention since the pioneering work by Haruta et al.<sup>1</sup> Au-nanoparticle-loaded TiO<sub>2</sub> (Au/TiO<sub>2</sub>) exhibits remarkable catalytic activity and selectivity toward a variety of reactions, such as low-temperature CO oxidation, partial oxidations of hydrocarbons, selective oxidations of alcohols, and hydrogenation.<sup>1–4</sup> More recently, it has also been reported that Au/TiO<sub>2</sub> could be used to realize visible-light-to-energy conversion<sup>5</sup> and could potentially be used in solar cells<sup>6,7</sup> and the photochemical elimination of organic contaminants.<sup>8</sup> In addition to the above approaches, we recently reported the first example of sonocatalysis by Au/TiO<sub>2</sub>.<sup>9</sup> Specifically, when supported on TiO<sub>2</sub>, 2-nm-diameter gold nanoparticles (NPs) exhibit high catalytic activity for the sonocatalytic degradation of organic dye pollutants.

Application of ultrasound in chemistry has been extensively studied, and commercial instruments for industrial purposes are readily available. Recently, more efficient catalysis has been realized through combination of ultrasonication with NPs.<sup>10–15</sup> Examples include the sonodegradation of organic pollutants catalyzed by TiO<sub>2</sub> NPs,<sup>10,11,14</sup> sonophotocatalysis by TiO<sub>2</sub>,<sup>11–15</sup> and sonocatalytic hydrogen production.<sup>16</sup> However, less attention has been paid to understanding the detailed mechanism of catalysis by metal oxides, particularly by noble-metal-NP-loaded metal oxides, in sonolysis.

On the other hand, noble-metal-NP-loaded metal oxides such as Au/TiO<sub>2</sub> and Pt/TiO<sub>2</sub> have also attracted much

attention in hydrogen production such as photocatalysis<sup>17–21</sup> and catalytic dehydrogenation.<sup>18,22,23</sup> In photocatalysis, to achieve high quantum yields, many model systems have included methanol as a sacrificial reagent to scavenge photogenerated holes and <sup>•</sup>OH radicals, an intermediate generated by the reaction of holes with water molecules.<sup>17–21</sup> However, reactions of methanol (and other sacrificial reagents) in these systems are rather complicated. Recent studies have shown that H<sub>2</sub> is also formed in the reforming of methanol over metal-loaded TiO<sub>2</sub> materials such as Au/TiO<sub>2</sub>, Pt/TiO<sub>2</sub>, Cu/TiO<sub>2</sub>, and Pd/TiO<sub>2</sub> under light irradiation.<sup>18,22,23</sup> Therefore, although sacrificial reagents are routinely used in hydrogen production, the pathways for hydrogen formation deserve careful consideration: How much of the evolved hydrogen is derived from water, and how important is each pathway for H<sub>2</sub> molecule formation? Both of these critical questions are also closely related to the function of Au NPs on the surface of TiO<sub>2</sub>. However, so far, neither question has been addressed in detail.

In this study, Au/TiO<sub>2</sub> was used for the first time in the sonocatalytic production of hydrogen, and the details of hydrogen evolution under various conditions were examined. Based on the detection of intermediate radicals, products of methanol, and isotopic compositions of evolved hydrogen, pathways for H<sub>2</sub> formation during catalyzed and noncatalyzed sonolysis are proposed, and the sources of hydrogen atoms in the evolved hydrogen gas are addressed. All of the evidence points to a mechanism whereby Au NPs on the TiO<sub>2</sub> surface significantly enhance both the thermal cleavage of water and the reforming of methanol in the gas phase of the cavitation bubbles.

\* To whom correspondence should be addressed. E-mail: jczhao@iccas.ac.cn. Fax and Tel.: +86-10-82616495.

<sup>†</sup> Chinese Academy of Sciences.

<sup>‡</sup> Queensland University of Technology.

## 2. Experimental Section

**2.1. Chemicals.** TiO<sub>2</sub> (P25, 80% anatase and 20% rutile; average diameter  $\approx$  21 nm, BET area  $\approx$  50 m<sup>2</sup> g<sup>-1</sup>) was purchased from Degussa Co. HAuCl<sub>4</sub>·4H<sub>2</sub>O (AR), activated Al<sub>2</sub>O<sub>3</sub> (for gas chromatography use, 60–80 mesh), methanol (AR), ethanol (AR), dimethyl sulfoxide (DMSO, AR), and glycerol (AR) were supplied by Sinopharm Chemical Reagent Beijing Co., Ltd. 5,5-Dimethyl-1-pyrroline-*N*-oxide (DMPO) and 3-carbamoyl-2,2,5,5-tetramethyl-1-pyrroline 1-oxide (CTMPO) were purchased from Sigma-Aldrich Co. D<sub>2</sub>O (99.9% D) was obtained from CIL Inc. H<sub>2</sub>, CO, and CH<sub>4</sub> standard gases were obtained from Beijing Hua Yuan Gas Chemical Industry Co., Ltd. Deionized water was used in all experiments.

**2.2. Methods.** Au NPs were loaded onto the surface of TiO<sub>2</sub> NPs (unless otherwise indicated, TiO<sub>2</sub> refers to Degussa P25 in this work) following the photoreduction method described previously<sup>9</sup> and summarized here. TiO<sub>2</sub> (1.0 g), methanol (0.50 mL), and a calculated amount of HAuCl<sub>4</sub> were dispersed in 100 mL of water in a Pyrex cylindrical bottle (final pH = 3.1). After the dispersion had been ultrasonicated for 15 min and stirred in the dark for 30 min, it was irradiated with a 500-W xenon lamp for 4 h to load Au nanoparticles onto the TiO<sub>2</sub>. Next, the dispersion was filtered, and the as-prepared catalyst was washed with water three times. Conversion of HAuCl<sub>4</sub> to Au(0) was tracked by UV–vis spectroscopy. The sonocatalytic activity of Au/TiO<sub>2</sub> increased with gold content and reached a plateau at  $\sim$ 0.5 wt % (Figure S1 in the Supporting Information). Therefore, Au/TiO<sub>2</sub> with 0.75 wt % Au was used for this study. The average diameter of the Au NPs was  $2.0 \pm 0.5$  nm as measured by transmission electron microscopy.<sup>9</sup> Citrate-stabilized Au NPs ( $3.5 \pm 0.7$  nm in diameter) were also prepared according to the literature method.<sup>24</sup>

Sonolysis reactions were carried out using a commercial 40-kHz transducer (UP2200H, Nanjing Panda Electronics Co. Ltd.) operating at 50 W. According to a calorimetric method,<sup>25</sup> the average power intensity of ultrasound was 0.045 W/mL. The reaction temperature was maintained at 21–25 °C using circulating water. Because rates of hydrogen evolution increased with Au/TiO<sub>2</sub> dosage and reached a plateau level at  $\sim$ 0.3 g L<sup>-1</sup> (Figure S2 in the Supporting Information), 0.5 and 1.0 g L<sup>-1</sup> catalyst dosages were chosen. A 250 mL Pyrex flask that was filled with 150 mL of the reactants and fixed close to the transducer was used as the reactor. The flask was sealed with a rubber stopper and purged with Ar for 30 min before each reaction. Unless otherwise emphasized, all reactions were performed under Ar.

For electron spin resonance (ESR, Bruker E500) experiments, 5 mL of water containing 5 mg of catalyst and 8 mM DMPO was irradiated with ultrasound; an Ar flow was maintained to keep the system isolated from air. After a certain regular interval, an aliquot was taken for EPR measurements immediately after sampling. Great care was taken to minimize experimental errors. Key parameters are as follows: center field = 3480 G, sweep width = 150.0 G, microfrequency = 9.77 GHz, and power = 12.6 mW. The WinSim program<sup>26</sup> was used for spectral simulation. Concentrations of DMPO–OH and DMPO–H were calculated based on the standard calibration curve of peak area vs concentration of CTMPO.<sup>27</sup>

Quantification of the evolved gas was performed with a gas chromatograph (GC, Techcomp GC7890) equipped with a thermal conductivity detector (TCD). A 5-Å molecular sieve packed column [3 m (length)  $\times$  3 mm (o.d.)  $\times$  2 mm (i.d.)] with Ar as the carrier gas was used to separate H<sub>2</sub>, CH<sub>4</sub>, and CO. To quantify H<sub>2</sub>, HD, and D<sub>2</sub>, a column [2 m (length)  $\times$  3

**TABLE 1: Rates ( $\mu$ mol h<sup>-1</sup>) of H<sub>2</sub> Evolution in Sonolysis Reactions<sup>a</sup>**

catalyst	water	methanol/ water <sup>b</sup>	ethanol/ water <sup>c</sup>	glycerol/ water <sup>d</sup>	DMSO/ water <sup>d</sup>
no catalyst	0.4	3.4	0.8	1.0	2.8
TiO <sub>2</sub>	1.3	15.1	25.0	9.5	12.8
Au/TiO <sub>2</sub>	21.6	282.3	198.1	31.4	39.1

<sup>a</sup> Catalyst dosage = 0.5 g L<sup>-1</sup>. <sup>b</sup> 4% (v/v). <sup>c</sup> 1.9% (v/v). <sup>d</sup> 0.67% (v/v).<sup>29</sup>

mm (o.d.)  $\times$  2 mm (i.d.)] packed with Fe<sub>2</sub>O<sub>3</sub>-modified activated Al<sub>2</sub>O<sub>3</sub> was prepared following the published method<sup>28</sup> with some optimization. The protocol for modifying activated Al<sub>2</sub>O<sub>3</sub> with Fe<sub>2</sub>O<sub>3</sub> is summarized as follows: FeCl<sub>3</sub> solution (30 mL, 0.139 mol) was added dropwise to a dispersion of active Al<sub>2</sub>O<sub>3</sub> (60 mL, 0.368 mol) under vigorous stirring; meanwhile, 4 M ammonium hydroxide was added to keep the pH between 3 and 4. Next, another 10 mL of concentrated ammonium hydroxide solution ( $\sim$ 14 M) was added. More water was added when the dispersion turned viscous. The dispersion was stirred for 2 h, filtered, washed three times, and dried under reduced pressure. The solid material was dried at 120 °C for 24 h, was then rescreened to 60–100 mesh, and finally was calcined at 500 °C for 4 h to convert Fe(OH)<sub>3</sub> into Fe<sub>2</sub>O<sub>3</sub>. For the separation of H<sub>2</sub>, HD, and D<sub>2</sub> by GC, temperatures of the inlet and the detector were both set to 50 °C; liquid nitrogen was used to maintain the temperature of the column (77 K), and highly purified Ne was used as the carrier gas. A typical chromatogram is shown in Figure S3 in the Supporting Information. D<sub>2</sub> standard gas was obtained by reaction of D<sub>2</sub>O with Na metal. Because HD standard gas was unavailable, the algebraic average of the correction factors of H<sub>2</sub> and D<sub>2</sub> was used for quantifying HD. Formaldehyde in aqueous solutions was analyzed using the acetylacetone spectrophotometric method.

## 3. Results and Discussion

**3.1. H<sub>2</sub> Evolution Catalyzed by Au/TiO<sub>2</sub>.** Au-nanoparticle-loaded TiO<sub>2</sub> (Au/TiO<sub>2</sub>) was used in sonocatalytic H<sub>2</sub> production. Very fast H<sub>2</sub> evolution from water (21.6  $\mu$ mol h<sup>-1</sup>; see Table 1) was obtained in the presence of Au/TiO<sub>2</sub> during sonolysis, whereas in the presence of bare P25 TiO<sub>2</sub>, H<sub>2</sub> evolution was much slower (1.3  $\mu$ mol h<sup>-1</sup>), and in the absence of any catalyst, the rate was extremely low (0.37  $\mu$ mol h<sup>-1</sup>). It should be noted here that no H<sub>2</sub> was detected without ultrasound, indicating that H<sub>2</sub> formation was caused by ultrasound rather than by indoor light. The effect of Au/TiO<sub>2</sub> was further examined in sonolysis of aqueous solutions of methanol, ethanol, glycerol, and DMSO, which are known to scavenge hydroxyl radicals and have been used as sacrificial reagents in H<sub>2</sub> production.<sup>17–21</sup> Au/TiO<sub>2</sub> significantly accelerated H<sub>2</sub> evolution in all of these cases, as expected. For example, compared to bare TiO<sub>2</sub>, Au/TiO<sub>2</sub> accelerated H<sub>2</sub> evolution by 18-fold using a 4% (v/v) methanol/water solution. Clearly, Au/TiO<sub>2</sub> increased the energy efficiency of the ultrasonic treatment.

In the absence of a catalyst, the rate of H<sub>2</sub> evolution during sonolysis of pure water (0.37  $\mu$ mol h<sup>-1</sup>; see Table 1) was close to that reported by Sasikala et al.,<sup>16</sup> where a total amount of  $\sim$ 0.14  $\mu$ mol of H<sub>2</sub> was evolved within 50 min, showing that the experimental conditions were similar. However, the present Au/TiO<sub>2</sub> was  $\sim$ 20 times more effective than the previously reported (metal oxide) catalyst.<sup>16</sup> The enhancement of catalytic activity by Au loading also far exceeds the negative effect of a (modest) size increase that, according to Sasikala et al.,<sup>16</sup> might reduce the activity of the catalyst. Actually, as far as we know,

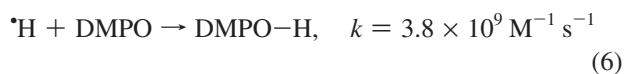
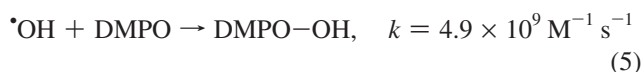
Au/TiO<sub>2</sub> has been the most efficient sonocatalyst for both H<sub>2</sub> formation and degradation of azo dyes.<sup>9</sup>

Data in Table 1 also show that methanol and ethanol were more efficient sacrificial reagents for H<sub>2</sub> evolution than glycerol and DMSO when Au/TiO<sub>2</sub> was used as the sonocatalyst. In contrast, in the presence of bare TiO<sub>2</sub> or in the absence of any catalyst, although the four sacrificial reagents also accelerated H<sub>2</sub> evolution, any differences in their effects on H<sub>2</sub> evolution were insignificant. This shows that the activity of Au/TiO<sub>2</sub> in sonocatalytic H<sub>2</sub> production strongly depends on the volatility of the sacrificial reagents.

To examine the stability of Au/TiO<sub>2</sub>, three repeated runs of the reaction were performed (Supporting Information, Figure S4) in which H<sub>2</sub> evolution retained a high and reproducible rate. The total turnover number (TTN, molecules of H<sub>2</sub> per atom of surface-loaded Au) reached 506 (mol H<sub>2</sub>/mol Au) within 15 h. These results indicate that Au/TiO<sub>2</sub> was very stable under our experimental conditions, in agreement with a previous study.<sup>9</sup>

Control experiments showed that (3.5 ± 0.7)-nm-diameter citrate-stabilized Au NPs<sup>24</sup> alone exhibited little sonocatalytic activity (data not shown). When citrate-stabilized Au NPs and bare TiO<sub>2</sub> were both used in the sonolysis of a 4.0 vol % methanol solution, the H<sub>2</sub> evolution rate was 14.5 μmol h<sup>-1</sup>, close to that of bare TiO<sub>2</sub> (Table 1), suggesting that Au NPs have a high sonocatalytic activity for H<sub>2</sub> evolution only when attached to the TiO<sub>2</sub> surface.

**3.2. Detection of Radicals during Sonolysis.** The propagation of ultrasonic waves through water causes numerous tiny cavitation bubbles, which, during collapse, produce local “hot spots” of high temperature and high pressure (e.g., 5000 K, 1000 atm).<sup>30</sup> Under these extreme conditions, water molecules undergo homolytic cleavage and form <sup>•</sup>OH and H<sup>•</sup> radicals (eq 1). Subsequent recombination of <sup>•</sup>OH and H<sup>•</sup> radicals gives rise to H<sub>2</sub> and H<sub>2</sub>O<sub>2</sub> (eqs 2–4).<sup>11,31</sup> A spin trap such as DMPO can be used to capture the radicals, resulting in the formation of long-lived spin adducts (eqs 5 and 6;<sup>32</sup> Figure S5 in the Supporting Information) that can be detected by the electron spin resonance (ESR) spectroscopy. As shown in Figure 1, DMPO–OH has a characteristic four-line hyperfine structure (peak height ratio 1:2:2:1, curve a), DMPO–H has nine lines (curve b), and a mixture of the two spin adducts is also composed of nine lines (curves c and d).



Both <sup>•</sup>OH and H<sup>•</sup> radicals were generated in the sonolysis of water in the presence of Au/TiO<sub>2</sub>, in the presence of bare TiO<sub>2</sub>,

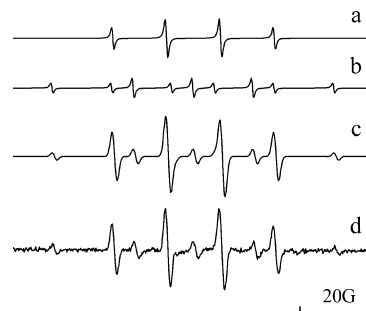


**Figure 1.** Simulated spectra of (a) DMPO–OH, (b) DMPO–H, and (c) a mixture of the two and (d) observed ESR signals.

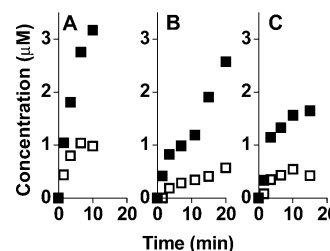


**Figure 2.** Evolution of (■) DMPO–OH and (□) DMPO–H by sonolysis of water (A) in the presence of Au/TiO<sub>2</sub>, (B) in the presence of bare TiO<sub>2</sub>, and (C) in the absence of a catalyst.<sup>33</sup> Conditions: Ar atmosphere, catalyst dosage of 1 g L<sup>-1</sup>.

and in the absence of a catalyst (Figure 2). In the presence of Au/TiO<sub>2</sub>, average rates of formation of DMPO–OH and DMPO–H within the first 10 min were 0.32 and 0.12 μM min<sup>-1</sup>, respectively, whereas in the presence of bare TiO<sub>2</sub>, the corresponding rates were 0.11 and 0.033 μM min<sup>-1</sup>. Because recombination of two H<sup>•</sup> radicals forms a H<sub>2</sub> molecule (eq 3), a higher rate of formation of H<sup>•</sup> in the presence of Au/TiO<sub>2</sub> than in the presence of bare TiO<sub>2</sub> is consistent with the results in Table 1, which shows that Au/TiO<sub>2</sub> greatly accelerated H<sub>2</sub> formation from pure water. Therefore, Au/TiO<sub>2</sub> greatly enhanced the thermal cleavage of water (eq 1) in sonocatalysis. It can also be seen from Figure 2 that bare TiO<sub>2</sub> actually enhanced the thermal cleavage of water, too, compared to the noncatalytic system.

Complex mixtures of radicals were formed by the sonolysis of methanol/water mixtures under Ar atmosphere. These radicals included H<sup>•</sup>, <sup>•</sup>OH, <sup>•</sup>CH<sub>3</sub>, and <sup>•</sup>CH<sub>2</sub>OH (see Supporting Information, Figure S6, for a typical ESR spectrum). The ESR spectra were fitted with the WinSim program, and concentrations of DMPO–OH and DMPO–H were extracted. Yields of DMPO–OH and DMPO–H within the first 10 min of sonolysis and rates of H<sub>2</sub> formation are plotted as functions of methanol concentration in Figure 3. At low methanol concentration [e.g., <10% (v/v)], both spin adducts were detected. The yield of DMPO–OH decreased sharply with methanol concentration, whereas the yield of DMPO–H decreased only slowly with methanol concentration. The rate of H<sub>2</sub> evolution increased steeply with methanol concentration when the methanol concentration was lower than ~5% (v/v), reaching a maximum at ~5% (v/v) and gradually decreasing with any further increase in methanol concentration.

One important reason for the large enhancement of H<sub>2</sub> evolution upon addition of methanol at methanol concentrations lower than 5% (v/v) (Figure 3) is that methanol efficiently captures <sup>•</sup>OH radicals (eq 7<sup>34</sup>), resulting in the effective inhibition of recombination between <sup>•</sup>OH and H<sup>•</sup> (eq 2). This can be understood in terms of the high volatility of methanol and the large rate constant associated with the reaction between



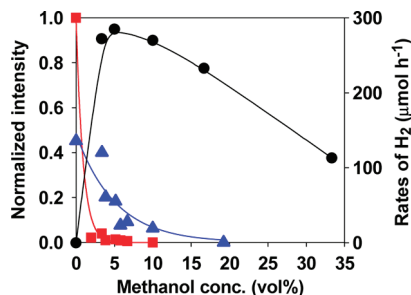


**Figure 3.** Formation of (■) DMPO–OH and (▲) DMPO–H after 10 min of sonolysis of water in the presence of Au/TiO<sub>2</sub> (0.5 g/L) and (●) rate of H<sub>2</sub> evolution as functions of methanol concentration.

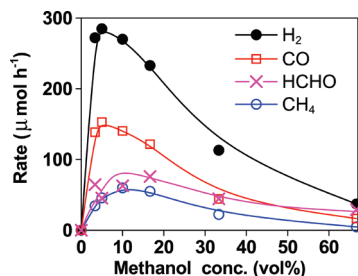


**Figure 4.** Rates of formation of major products in the sonolysis of water/methanol mixtures in the presence of Au/TiO<sub>2</sub> (0.5 g/L).

methanol and  $\cdot\text{OH}$  (eq 7): Efficient scavenging of  $\cdot\text{OH}$  by methanol occurs both in the interior and in the interfacial zone of the cavitation bubbles (see section 3.5). Further, the yield of DMPO–OH depends not only on the concentration of DMPO, but also on the concentration of other  $\cdot\text{OH}$  scavengers. A rough calculation illustrated in Figure S7 (Supporting Information) shows that the fraction of  $\cdot\text{OH}$  scavenged by DMPO decreased drastically with increasing methanol concentration. Our experimental observations (Figure 3) showed that the yield of DMPO–OH declined in line with a similar trend, but faster than the calculated results. In contrast to DMPO–OH, the weaker dependence of the yield of DMPO–H on methanol concentration (Figure 3) can be attributed to the inefficient scavenging of  $\cdot\text{H}$  by methanol (eq 8<sup>34</sup>), which is consistent with the calculated results (Supporting Information, Figure S7).



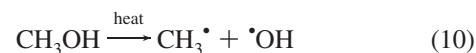
$$k = 9.7 \times 10^8 \text{ M}^{-1} \text{ s}^{-1} \quad (7)$$



$$k = 2.6 \times 10^6 \text{ M}^{-1} \text{ s}^{-1} \quad (8)$$

**3.3. Products of Methanol during Sonolysis.** Four major products, namely, H<sub>2</sub>, CO, HCHO, and CH<sub>4</sub>, were detected in the sonolysis of water/methanol mixtures under Ar atmosphere<sup>35</sup> in the presence of Au/TiO<sub>2</sub>. Their formation rates varied similarly with the methanol concentration, that is, they all first increased steeply, passing through peak values at ~5% (v/v) of methanol (Figure 4).

During sonication, HCHO was formed by H-abstraction of methanol mainly by  $\cdot\text{OH}$  and  $\text{H} \cdot$  radicals (eq 9).<sup>35,36</sup> Meanwhile thermal cleavage of methanol generated methyl radicals which then formed CH<sub>4</sub> (eq 10).<sup>35,36</sup> Nevertheless, the four major products, H<sub>2</sub>, CO, HCHO and CH<sub>4</sub>, were actually derived from both oxidation (by  $\cdot\text{OH}$  and  $\text{H} \cdot$  by water cleavage, eq 1) and thermal reforming of methanol.



The catalytic activity of Au NPs on the TiO<sub>2</sub> surface was then investigated by comparing the products of methanol in the sonolysis of methanol solutions in the presence of Au/TiO<sub>2</sub>, bare TiO<sub>2</sub>, and in the absence of a catalyst (Figure 4 and Figure S8 in the Supporting Information). As in the Au/TiO<sub>2</sub> system, the formation rates of H<sub>2</sub>, CO, HCHO, and CH<sub>4</sub> in the other two systems also increased with methanol concentration and passed through their maxima at ~5% (v/v) methanol. At the methanol concentration for the fastest H<sub>2</sub> evolution, the ratio of the rates of H<sub>2</sub>, CO, HCHO, and CH<sub>4</sub> was 1.0:0.53:0.16:0.16 for Au/TiO<sub>2</sub>, 1.0:0.51:0.22:0.14 for bare TiO<sub>2</sub>, and 1.0:0.54:0.22:0.15 without a catalyst. The ratio of HCHO (to H<sub>2</sub>) for the Au/TiO<sub>2</sub> system was lower, whereas the ratio of CH<sub>4</sub> (to H<sub>2</sub>) was slightly higher than those of the other two systems. It can also be seen that the ratios of CO (to H<sub>2</sub>) in the three systems were close to one other. Numerous reports showed that 2–3-nm Au NPs attached to TiO<sub>2</sub> surfaces exhibited high catalytic activity for CO oxidation.<sup>3,4</sup> In the present work, carried out under Ar (i.e., no dioxygen was present), the selective oxidation of CO was not observed.

**3.4. Tracking the Source of Hydrogen with H/D Isotope Evidence.** Based on analysis of intermediate radicals and products during the sonolysis of methanol solutions, three pathways are proposed for the formation of dihydrogen (H<sub>2</sub>). These are pathway 1, the recombination of two  $\text{H} \cdot$  atoms formed by the cleavage of water molecules; pathway 2, H-abstraction from methanol by  $\text{H} \cdot$  generated by water cleavage; and pathway 3, thermal reforming of methanol. In this section, the relative importance of each pathway is assessed. This was done by analyzing hydrogen-isotope compositions of the H<sub>2</sub> gas evolved from methanol solutions containing deuterated reagents. As a prerequisite, the effect of ultrasound on the hydrogen-isotope composition of the gas phase had to be examined. To do this, a small amount of H<sub>2</sub> (or D<sub>2</sub>) gas was deliberately added to the headspace of the reactor prior to sonolysis (see Figure S9 and the discussion in the Supporting Information). Under ultrasound irradiation, the product of H/D isotopic exchange, HD, was effectively undetectable; as the reaction was prolonged, the headspace of the reactor was actually filled with a mixture of H<sub>2</sub>, D<sub>2</sub>, and Ar, but still no HD was detected. This and other evidence<sup>37</sup> indicates that H/D exchange of hydrogen in the gas phase should be ignored under the present experimental conditions. Therefore, the isotope profile of each gas (i.e., H<sub>2</sub>, HD, and D<sub>2</sub>) was used to calculate its rate of formation during sonolysis of solutions of CH<sub>3</sub>OH/D<sub>2</sub>O or CD<sub>3</sub>OD/H<sub>2</sub>O in the presence of Au/TiO<sub>2</sub>, in the presence of bare TiO<sub>2</sub>, and in the absence of a catalyst.

As can be seen in Figure 5, the amount of each gas increased linearly with reaction time. The average rates ranged from 57  $\mu\text{mol h}^{-1}$  for HD, to 37  $\mu\text{mol h}^{-1}$  for D<sub>2</sub> and to 16  $\mu\text{mol h}^{-1}$  for H<sub>2</sub> from a CD<sub>3</sub>OD/H<sub>2</sub>O solution (1:19 v/v, Figure 5A). The rates were 61, 35, and 22  $\mu\text{mol h}^{-1}$  for evolution of HD, H<sub>2</sub>, and D<sub>2</sub>, respectively, from a CH<sub>3</sub>OH/D<sub>2</sub>O solution (1:19 v/v, Figure 5B). These rates correspond to the three pathways for hydrogen molecule formation. H<sub>2</sub> in Figure 5A and D<sub>2</sub> in Figure 5B are the products of recombination of two  $\text{H} \cdot$  (or  $\text{D} \cdot$ ) radicals from water cleavage (pathway 1). HD in both panels is the

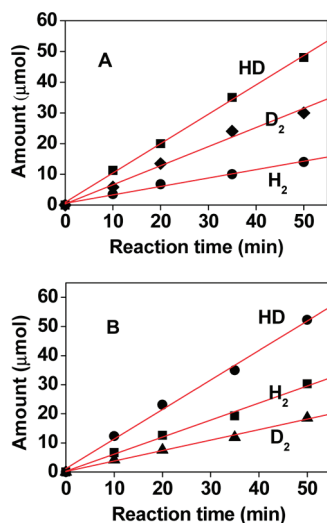


**Figure 5.** Formation of H<sub>2</sub>, D<sub>2</sub>, and HD by sonolysis of mixtures of (A) 19 mL of H<sub>2</sub>O and 1 mL of CD<sub>3</sub>OD and (B) 19 mL of D<sub>2</sub>O and 1 mL of CH<sub>3</sub>OH.<sup>38</sup> In both cases, Au/TiO<sub>2</sub> (1 g L<sup>-1</sup>) was used.

product of H-abstraction (or D-abstraction) of methanol by H<sup>•</sup> (or D<sup>•</sup>) from cleavage of water (pathway 2). D<sub>2</sub> in panel A and H<sub>2</sub> in panel B are the products of thermal reforming of methanol (pathway 3). The total rates of all three pathways in panels A and B of Figure 5 were close (110 vs 118 μmol h<sup>-1</sup>). This is reasonable, given that the deuterium kinetic effects become insignificant at the high temperatures [ $k_H/k_D = \exp(-\Delta E_d/RT)$  approaches 1 as  $T$  increases] of the hot spots caused by ultrasound.<sup>30</sup> The ratio of the three pathways in Figure 5A is 1.0:3.5:2.3 for pathway 1 to pathway 2 to pathway 3. This also indicates that the ratio of H-atoms from H<sub>2</sub>O to D-atoms from CD<sub>3</sub>OD is 0.7:1.0. In Figure 5B, the ratio of the three pathways is 1.0:2.8:1.6 for pathway 1 to pathway 2 to pathway 3; the ratio of D-atoms from D<sub>2</sub>O to H-atoms from CH<sub>3</sub>OH is 0.8:1.0. Under sonication, isotope exchange between methanol and water was expected to occur. We speculate that its rate should be of the same order of magnitude as that of hydrogen evolution, so that, with respect to the time scale of the experiments of Figure 5, the isotopic composition of the liquid phase could be regarded as unchanged. Therefore, the above data indicate that all three pathways are important for hydrogen formation. During the sonolysis of aqueous methanol in the presence of Au/TiO<sub>2</sub>, added methanol accelerated the rate of H<sub>2</sub> evolution by a factor of 12 (Table 1), but water was still an important source of hydrogen.

Analogously, sonolysis of CD<sub>3</sub>OD/H<sub>2</sub>O solutions in the presence of bare TiO<sub>2</sub> and in the absence of a catalyst was also performed (Supporting Information, Figure S10). The data indicated that pathway 3 was slightly more pronounced in the Au/TiO<sub>2</sub> system than in the other two systems, which suggested that the reforming of methanol was enhanced by Au NPs. Moreover, for both TiO<sub>2</sub> and noncatalytic systems, nearly half of the hydrogen atoms were also from water.

**3.5. Mechanism of Au/TiO<sub>2</sub>-Enhanced H<sub>2</sub> Evolution.** The chemical effects of ultrasound are brought about by the high temperature and pressure during the violent collapse of the cavitation bubbles. The microbubbles are tens to hundreds of micrometers in diameter<sup>30,39</sup> and are filled with dissolved gas and solvent vapor. The interiors of these bubbles have the highest temperature—ca. 5000 K.<sup>30</sup> The interfacial zone is a liquid layer ca. 200–300 nm thick<sup>30</sup> that surrounds the collapsing cavitation bubbles. The temperature of the interfacial zone

is over 1900 K.<sup>30</sup> The third region is the bulk solution, which is much less active.

Methanol is highly volatile and readily enters cavitation bubbles. It accelerates hydrogen evolution by capturing H<sup>•</sup> (eq 8) and scavenging <sup>•</sup>OH radicals (eq 7). Thermal reforming of methanol at the high temperatures present at the hot spots also generates H<sub>2</sub>. Other sacrificial reagents, such as ethanol, glycerol, and DMSO in Table 1, also accelerated hydrogen evolution to different extents. Among them, ethanol is physically and chemically similar to methanol. It not only captures <sup>•</sup>OH and H<sup>•</sup> radicals but also readily enters cavitation bubbles for pyrolysis. Glycerol and DMSO are good <sup>•</sup>OH scavengers but are much less volatile (the boiling point of glycerol is 290 °C, and that of DMSO is 189 °C). Thus at low concentrations, both accelerate H<sub>2</sub> evolution mainly by scavenging <sup>•</sup>OH radicals in the interfacial zone, whereas the thermal reforming favored in the interior of the cavitation bubbles does not contribute significantly to hydrogen formation.<sup>27</sup> Therefore, higher rates of hydrogen evolution with methanol or ethanol than with glycerol or DMSO (see Table 1) as the sacrificial reagents are attributed to the enhanced thermal reactions (e.g., thermal cleavage of water and reforming of the alcohols) in the interior of the cavitation bubbles. For example, the rate of H<sub>2</sub> evolution in the presence of Au/TiO<sub>2</sub> was about 9 times larger with methanol than with glycerol. Furthermore, this acceleration was more significant in the presence of Au/TiO<sub>2</sub> than in the presence of bare TiO<sub>2</sub> (an increase of less than 2-fold) and in the absence of a catalyst (less than 3 times as fast). Therefore, thermal reactions in the interior of the cavitation bubbles were greatly enhanced by Au/TiO<sub>2</sub>. This conclusion is also consistent with and supported by the facts that (1) hydrogen evolution was much faster by sonolysis of water in the presence of Au/TiO<sub>2</sub> than in the presence of bare TiO<sub>2</sub> and in the absence of a catalyst; (2) yields of <sup>•</sup>OH and H<sup>•</sup> were higher in the Au/TiO<sub>2</sub> system than in the other two systems; (3) deuterium isotope experiments indicated that, in all three systems, water was an important source of hydrogen; (4) deuterium isotope experiments also suggested that Au enhanced the thermal reforming of methanol; and (5) cleavage of water occurs mainly in the interior region, whereas the temperature of the interfacial zone (1900 K) is not high enough for water cleavage.<sup>40</sup>

The thickness of the interfacial zone of a cavitation bubble, 200–300 nm,<sup>30</sup> is 10–15 times the diameter of an individual TiO<sub>2</sub> NP (P25,  $d = 21$  nm). Taking into account that each TiO<sub>2</sub> aggregate contains tens of individual particles (aggregation is often observed when a metal oxide material is dispersed in water, e.g., Au/TiO<sub>2</sub> in ref 9), Au/TiO<sub>2</sub> and TiO<sub>2</sub> are likely to extend through interfacial zones to the interiors of cavitation bubbles, thereby creating solid–gas interfaces. These solid–gas interfaces are responsible for the sonocatalytic activity. Therefore, the higher sonocatalytic activity of Au/TiO<sub>2</sub> compared to bare TiO<sub>2</sub> could be attributed to the high catalytic activity of gold NPs for the thermal reforming of methanol and cleavage of water.<sup>41,42</sup> This also explains why other noble-metal NPs such as Pt NPs on TiO<sub>2</sub> also exhibit sonocatalytic activity for hydrogen evolution (Supporting Information, Figure S11).

#### 4. Conclusions

Au/TiO<sub>2</sub> greatly accelerates hydrogen evolution in the sonolysis of water and methanol solutions. To our knowledge, Au/TiO<sub>2</sub> is the most efficient sonocatalyst for H<sub>2</sub> formation and the degradation of azo dyes.<sup>9</sup> Three important pathways that are enhanced by using Au/TiO<sub>2</sub> are proposed for the formation of hydrogen molecules in aqueous methanol solutions. Although

the addition of methanol in the presence of Au/TiO<sub>2</sub> increased the rate of H<sub>2</sub> evolution by a factor of 12, nearly half of the hydrogen atoms were nevertheless derived from the water molecules. The high sonocatalytic activity of Au/TiO<sub>2</sub> can be attributed to its high activity for the thermal cleavage of water and the thermal reforming of methanol. The present study not only demonstrates the potential for applications of Au/TiO<sub>2</sub> in sonocatalysis, but also provides information relevant to understanding the mechanisms of hydrogen production in photocatalysis and catalytic dehydrogenation.

**Acknowledgment.** This work was supported by the 973 Project (2007CB613306), NFSC (20537010, 20777076, 20877076), and CAS. Y.W. thanks Prof. I. A. Weinstock for proofreading the manuscript.

**Supporting Information Available:** Chromatogram, data on H<sub>2</sub> evolution, analysis of ESR data, and more hydrogen isotope evidence. This material is available free of charge via the Internet at <http://pubs.acs.org>.

## References and Notes

- (1) Haruta, M.; Kobayashi, T.; Sano, H.; Yamada, N. *Chem. Lett.* **1987**, 405.
- (2) Daniel, M.; Astruc, D. *Chem. Rev.* **2004**, *104*, 293.
- (3) Valden, M.; Lai, X.; Goodman, D. W. *Science* **1998**, *281*, 1647.
- (4) Min, B. K.; Friend, C. M. *Chem. Rev.* **2007**, *107*, 2709.
- (5) Furube, A.; Du, L.; Hara, K.; Katoh, R.; Tachiya, M. *J. Am. Chem. Soc.* **2007**, *129*, 14852.
- (6) Tian, Y.; Tatsuma, T. *J. Am. Chem. Soc.* **2005**, *127*, 7632.
- (7) Yu, K.; Tian, Y.; Tatsuma, T. *Phys. Chem. Chem. Phys.* **2006**, *8*, 5417.
- (8) Chen, X.; Zhu, H.; Zhao, J.; Zheng, Z.; Gao, X. *Angew. Chem., Int. Ed.* **2008**, *47*, 5353.
- (9) Wang, Y.; Zhao, D.; Ma, W.; Chen, C.; Zhao, J. *Environ. Sci. Technol.* **2008**, *42*, 6173.
- (10) Wang, J.; Guo, B.; Zhang, X.; Zhang, Z.; Han, J.; Wu, J. *Ultrason. Sonochem.* **2005**, *12*, 331.
- (11) Adewuyi, Y. G. *Environ. Sci. Technol.* **2005**, *39*, 3409.
- (12) Harada, H. *Ultrason. Sonochem.* **2001**, *8*, 55.
- (13) Davydov, L.; Reddy, E. P.; France, P.; Smirniotis, P. G. *Appl. Catal. B: Environ.* **2001**, *32*, 95.
- (14) Adewuyi, Y. G. *Environ. Sci. Technol.* **2005**, *39*, 8557.
- (15) Berberidou, C.; Poullos, I.; Xekoukoulotakis, N. P.; Mantzavinos, D. *Appl. Catal. B: Environ.* **2007**, *74*, 63.
- (16) Sasikala, R.; Jayakumar, O. D.; Kulshreshtha, S. K. *Ultrason. Sonochem.* **2007**, *14*, 153.
- (17) Chen, D.; Ye, J. *Chem. Mater.* **2007**, *19*, 4585.
- (18) Wu, G.; Chen, T.; Su, W.; Zhou, G.; Zong, X.; Lei, Z.; Li, C. *Int. J. Hydrogen Energy* **2008**, *33*, 1243.
- (19) Lu, D.; Hara, M.; Hisatomi, T.; Takata, T.; Domen, K. *J. Phys. Chem. C* **2009**, *113*, 17151.
- (20) Higashi, M.; Abe, R.; Takata, T.; Domen, K. *Chem. Mater.* **2009**, *21*, 1543.
- (21) Yao, W.; Huang, C.; Ye, J. *Chem. Mater.* **2009**, *22*, 1107.
- (22) Meyer, S.; Saborowski, S.; Schäfer, B. *ChemPhysChem* **2006**, *7*, 572.
- (23) Bowker, M.; Millard, L.; Greaves, J.; James, D.; Soares, J. *Gold Bull.* **2004**, *37*, 170.
- (24) Jana, N. R.; Gearheart, L.; Murphy, C. J. *Langmuir* **2001**, *17*, 6782.
- (25) Wang, S.; Huang, B.; Wang, Y.; Liao, L. *Ultrason. Sonochem.* **2006**, *13*, 506.
- (26) Duling, D. R. *J. Magn. Reson. B* **1994**, *104*, 105.
- (27) Kondo, T.; Kirschenbaum, L. J.; Kim, H.; Riesz, P. *J. Phys. Chem.* **1993**, *97*, 522.
- (28) Zhou, J.; Gao, L. *Atom. Energy Sci. Technol.* **2007**, *41*, 356.
- (29) The volatility of DMSO is much lower than those of methanol and water. At [DMSO] < 20 vol %, the concentration of DMSO steam in the gas phase of the cavitation bubbles is low, and decomposition of DMSO occurs mainly by <sup>•</sup>OH attack in the interfacial zone (see ref 27). The rate of this reaction increases with the concentration of DMSO and reaches the maximum at [DMSO] = 0.2 vol %. Therefore, 0.67 vol % (instead of 4.0 vol %) DMSO was used. With the same consideration, 0.67 vol % glycerol was also used.
- (30) Suslick, K. S.; Hammerton, D. A.; Cline, R. E. *J. Am. Chem. Soc.* **1986**, *108*, 5641.
- (31) Halstead, C. J.; Jenkins, D. R. *Combust. Flame* **1970**, *14*, 321.
- (32) Faraggi, M.; Carmichael, A.; Riesz, P. *Int. J. Radiat. Biol. Relat. Stud. Phys., Chem. Med.* **1984**, *46*, 703.
- (33) Although H<sub>2</sub>O is split into <sup>•</sup>OH and <sup>•</sup>H radicals in a 1:1 ratio (eq 1), the measured ratio of the concentrations of DMPO-<sup>•</sup>OH and DMPO-<sup>•</sup>H is ~3:1. Similar results were also found in the following works: Makino, K.; Mossoba, M. M.; Riesz, P. *J. Phys. Chem.* **1983**, *87*, 1369. Makino, K.; Mossoba, M. M.; Riesz, P. *J. Am. Chem. Soc.* **1982**, *104*, 3537. This can be explained by the higher reactivity of <sup>•</sup>OH with DMPO and other species and by the longer lifetime of DMPO-<sup>•</sup>OH.
- (34) Buxton, G. V.; Greenstock, C. L.; Helman, W. P.; Ross, A. B. *J. Phys. Chem. Ref. Data* **1988**, *17*, 513.
- (35) Buettner, J.; Gutierrez, M.; Henglein, A. *J. Phys. Chem.* **1991**, *95*, 1528.
- (36) Krishna, C. M.; Lion, Y.; Kondo, T.; Riesz, P. *J. Phys. Chem.* **1987**, *91*, 5847.
- (37) Fischer, C. H.; Hart, E. J.; Henglein, A. *J. Phys. Chem.* **1986**, *90*, 222.
- (38) The non-symmetrical results in panels A and B could be due to (1) small differences in methanol concentrations, arising from changes in the densities of H<sub>2</sub>O, D<sub>2</sub>O, CH<sub>3</sub>OH, and CD<sub>3</sub>OD (1.00, 1.11, 0.78, and 0.89 g mL<sup>-1</sup>, respectively) and (2) a small kinetic isotope effect.
- (39) Hung, H.; Hoffmann, M. R. *J. Phys. Chem. A* **1999**, *103*, 2734.
- (40) Baykara, S. Z. *Int. J. Hydrogen Energy* **2004**, *29*, 1459.
- (41) Haruta, M.; Ueda, A.; Tsubota, S.; Torres Sanchez, R. M. *Catal. Today* **1996**, *29*, 443.
- (42) Nuhu, A.; Jorge, S.; Monica, G.; Andrew, W.; Ghulam, H.; Bowker, M. *Top. Catal.* **2007**, *44*, 293.

JP105691V